



HAL
open science

Estimation of the fuzzy structure parameters for continuous junctions

Christian Soize, K. Bjaoui

► **To cite this version:**

Christian Soize, K. Bjaoui. Estimation of the fuzzy structure parameters for continuous junctions. Journal of the Acoustical Society of America, 2000, 107 (4), pp.2011-2020. 10.1121/1.428485. hal-00765557

HAL Id: hal-00765557

<https://hal.science/hal-00765557>

Submitted on 14 Dec 2012

HAL is a multi-disciplinary open access archive for the deposit and dissemination of scientific research documents, whether they are published or not. The documents may come from teaching and research institutions in France or abroad, or from public or private research centers.

L'archive ouverte pluridisciplinaire **HAL**, est destinée au dépôt et à la diffusion de documents scientifiques de niveau recherche, publiés ou non, émanant des établissements d'enseignement et de recherche français ou étrangers, des laboratoires publics ou privés.

ESTIMATION OF FUZZY STRUCTURE PARAMETERS FOR CONTINUOUS JUNCTIONS

Christian Soize and Karina Bjaoui

*Structural Dynamics and Coupled Systems Department, ONERA, BP 72, 92322 Chatillon
Cedex, France*

ABSTRACT

The fuzzy structure theory introduced fifteen years ago is designed to predict the frequency response functions of structures and structural acoustic systems with structural complexity, in the low- and medium-frequency ranges. This paper constitutes a first validation of the fuzzy structure theory for continuous junctions between the master structure and the fuzzy substructures. In addition, we present a method to estimate the fuzzy structure parameters introduced in the fuzzy structure theory and we validate it for the case of continuous junctions. This validation obtained by numerical simulations opens the field of experimental identifications.

PACS numbers: 43.40

INTRODUCTION

The fuzzy structure theory was introduced by Soize¹ in order to model structural complexity in the medium frequency range. This structural complexity plays a fundamental role in the response of a master structure coupled with complex substructures in the context of structural-acoustic systems. In 1993, a second fuzzy impedance law was proposed² to model the case of fuzzy substructures attached to the master structure through a continuous junction. Since 1993, much research has been published concerning the problem of a master structure coupled with a large number of simple linear oscillators³⁻¹⁸ and a few concerning continuous cases¹⁹⁻²². Two main problems had to be solved to be able to apply the fuzzy structure theory (described in detail in Ref. 23) to the case of continuous junctions. The first problem was related to the construction of a procedure for identifying the fuzzy structure parameters in order to solve complex problems and to allow experimental identifications to be performed. The second one, which requires solving the first, is related to validation of the fuzzy structure

theory for continuous junctions. A general procedure has been developed²⁴ to solve the first problem. In this paper, we present a first validation of the fuzzy structure theory for continuous junctions between the master structure and the fuzzy substructures. We introduce a new cost function replacing the cost function previously introduced²⁴. It allows an efficient estimation of the fuzzy structure parameters using a procedure based on the statistical energy approach. In Section I, we introduce the reference complex structure, its model and the numerical simulation of its response. All the validations are performed with respect to this reference. Section II deals with modeling of the reference complex structure using the fuzzy structure theory. In Section III, we present the procedure for estimating the fuzzy structure mean parameters. Finally, the last section is devoted to validation by comparison with reference results.

I. REFERENCE COMPLEX STRUCTURE MODEL AND NUMERICAL SIMULATION OF ITS RESPONSE

The complex structure consists of a master structure coupled with four complex substructures (see Figure 1). The master structure is constituted of two rectangular homogeneous isotropic thin plates denoted as (1) and (2), in bending mode and simply supported. Plate (1) is coupled to plate (2) along their common edge; the rotation around this edge is continuous. The complex substructures are denoted as (a), (b), (c) and (d) and are constituted of a rectangular homogeneous isotropic thin plate on which many simple linear oscillators are attached. The plate of each complex substructure is in bending mode, simply supported and coupled to a plate of the master structure along their common edge; the rotation around this edge is continuous. Consequently, there is a continuous junction between each complex substructure and the master structure. Two plates belonging to different complex substructures are not coupled along their common edge (there is coupling only between each complex substructure and the master structure). The method used to construct the model of the reference complex structure consists in constructing the generalized impedance matrix of an isolated plate belonging to the master structure and an isolated complex substructure. Then the isolated subsystems constituting the reference complex structure are coupled using a Lagrange multiplier technique in order to express the continuity of the rotation on the junctions.

A. Generalized impedance matrix of an isolated plate belonging to the master structure

Each rectangular thin plate (r) (with r equal to 1 or 2) of the master structure is referenced to an (x, y) local coordinate system and is located in plane Oxy . This plate has a constant thickness, a length L_{r1} , a width L_{r2} , surface-mass density ρ_r (mass per unit area), a constant damping rate ξ_r and a constant flexural rigidity D_r . The domain of this plate (middle surface) is defined by $\Omega_r =]0, L_{r1}[\times]0, L_{r2}[$. We consider linear vibrations of this plate formulated in the frequency domain ω . The transverse displacement of plate (r) in a point (x, y) is denoted as $u_r(\omega, x, y)$. The external forces applied to the plate are represented by a complex-valued function $f_r(\omega, x, y)$. The bending moment around the edges of plate (r) is denoted as $\mathcal{M}_{\mathbf{n}_r}$ in which \mathbf{n}_r is the outward unit normal to the boundary $\partial\Omega_r$ of domain Ω_r . The boundary value problem is written as

$$\begin{aligned} -\omega^2 \rho_r u_r - 2i\omega \xi_r \{\rho_r D_r\}^{1/2} \nabla^2 u_r + D_r \nabla^4 u_r &= f_r \quad \text{in } \Omega_r \quad , \\ u_r &= 0 \quad \text{on } \partial\Omega_r \quad , \\ \mathcal{M}_{\mathbf{n}_r} &= 0 \quad \text{on } \partial\Omega_r \quad . \end{aligned} \quad (1)$$

The boundary value problem defined by Eq. (1) is solved using the Ritz-Galerkin method for which the complete family of independent functions in the admissible function space is constituted of the normal modes related to the simply supported plate. We then introduce the normal modes²⁵

$$\varphi_{r\beta}(x, y) = \frac{2}{\sqrt{L_{r1}L_{r2}}} \sin\left(\frac{\beta_1\pi x}{L_{r1}}\right) \sin\left(\frac{\beta_2\pi y}{L_{r2}}\right) \quad , \quad (2)$$

and the corresponding eigenfrequencies

$$\omega_{r\beta} = \sqrt{\frac{D_r}{\rho_r}} \left\{ \left(\frac{\beta_1\pi}{L_{r1}}\right)^2 + \left(\frac{\beta_2\pi}{L_{r2}}\right)^2 \right\} \quad , \quad (3)$$

in which $\beta = (\beta_1, \beta_2)$ where β_1 and β_2 are positive integers. The finite dimension approximation of field u_r is written as $\tilde{u}_r(\omega, x, y) = \sum_{\beta \in \mathcal{B}^r} q_{r\beta}(\omega) \varphi_{r\beta}(x, y)$ in which \mathcal{B}^r is the set of all the pairs of integers (β_1, β_2) such that $\tilde{u}_r(\omega, x, y)$ approaches $u_r(\omega, x, y)$. Let $\mathbf{q}_r(\omega)$ and $\mathbf{f}_r(\omega)$ be the vectors of generalized coordinates and generalized forces such that

$$\mathbf{q}_r(\omega) = \{q_{r\beta}(\omega)\}_{\beta \in \mathcal{B}^r} \quad , \quad \mathbf{f}_r(\omega) = \{f_{r\beta}(\omega)\}_{\beta \in \mathcal{B}^r} \quad , \quad (4)$$

in which $f_{r\beta}(\omega) = \int_0^{L_{r1}} \int_0^{L_{r2}} f_r(\omega, x, y) \varphi_{r\beta}(x, y) dx dy$. Consequently, for all real ω , vector $\mathbf{q}_r(\omega)$ is the solution of the complex matrix equation $i\omega [Z_r(\omega)] \mathbf{q}_r(\omega) = \mathbf{f}_r(\omega)$ in which $[Z_r(\omega)]$ is the generalized impedance complex diagonal matrix such that

$$i\omega [Z_r(\omega)]_{\beta\beta'} = \rho_r \{-\omega^2 + 2i\omega \xi_r \omega_{r\beta} + \omega_{r\beta}^2\} \delta_{\beta\beta'} \quad , \quad (5)$$

with $\delta_{\beta\beta'} = 1$ if $\beta = \beta'$ and $= 0$ otherwise.

B. Generalized impedance matrix of an isolated complex substructure

Each complex substructure (s) (with s equal to a, b, c or d) is constituted of a rectangular thin plate (s) on which K_s simple linear oscillators are attached. Plate (s) is referenced to an (x, y) local coordinate system and is located in plane Oxy . This plate has a constant thickness, a length L_{s1} , a width L_{s2} , a surface-mass density ρ_s (kg/m²), a constant damping rate ξ_s and a constant flexural rigidity D_s . The domain of this plate (middle surface) is defined by $\Omega_s =]0, L_{s1}[\times]0, L_{s2}[$. We consider linear vibrations of this complex substructure formulated in the frequency domain ω . The transverse displacement of the plate (s) in a point (x, y) is denoted as $u_s(\omega, x, y)$. The external forces applied to the plate are represented by a complex-valued function $f_s(\omega, x, y)$. The bending moment around the edges of plate (s) is denoted as $\mathcal{M}_{\mathbf{n}_s}$ in which \mathbf{n}_s is the outward unit normal to the boundary $\partial\Omega_s$ of domain Ω_s . The mass, damping rate and stiffness of the κ -th simple linear oscillator ($\kappa = 1, \dots, K_s$) attached to plate (s) are constant and denoted as m_s^κ , ξ_s^κ and $m_s^\kappa (\omega_s^\kappa)^2$ respectively (ω_s^κ is the eigenfrequency of the undamped oscillator with a fixed support). Oscillator κ is located in point (x^κ, y^κ) . The area of the plate of the complex substructure is divided into $\sqrt{K_s}$ subelements (rectangular subelement) and $\sqrt{K_s}$ oscillators are uniformly distributed in space inside each subelement and in frequency inside the frequency band of analysis. The boundary value problem is written as

$$\begin{aligned} -\omega^2 \rho_s u_s - 2i\omega \xi_s (\rho_s D_s)^{1/2} \nabla^2 u_s + D_s \nabla^4 u_s &= f_s - \sum_{\kappa=1}^{K_s} g_s^\kappa \quad \text{in } \Omega_s \quad , \\ u_s &= 0 \quad \text{on } \partial\Omega_s \quad , \\ \mathcal{M}_{\mathbf{n}_s} &= 0 \quad \text{on } \partial\Omega_s \quad . \end{aligned} \quad (6)$$

Force $g_s^\kappa(\omega)$ induced by oscillator κ is such that

$$g_s^\kappa(\omega) = i\omega z_s^\kappa(\omega) u_s(\omega, x^\kappa, y^\kappa) \quad , \quad (7)$$

in which z_s^κ is such that

$$i\omega z_s^\kappa(\omega) = -\omega^2 \left(\frac{m_s^\kappa (\omega_s^\kappa/\omega)^2 ((\omega_s^\kappa/\omega)^2 - 1 + 4(\xi_s^\kappa)^2)}{((\omega_s^\kappa/\omega)^2 - 1)^2 + 4(\omega_s^\kappa/\omega)^2(\xi_s^\kappa)^2} \right) + i\omega \left(\frac{2m_s^\kappa \omega \xi_s^\kappa (\omega_s^\kappa/\omega)}{((\omega_s^\kappa/\omega)^2 - 1)^2 + 4(\omega_s^\kappa/\omega)^2(\xi_s^\kappa)^2} \right). \quad (8)$$

The boundary value problem defined by Eq. (6) is solved similarly to Eq. (1), introducing the normal modes,

$$\varphi_{s\beta}(x, y) = \frac{2}{\sqrt{L_{s1}L_{s2}}} \sin\left(\frac{\beta_1\pi x}{L_{s1}}\right) \sin\left(\frac{\beta_2\pi y}{L_{s2}}\right), \quad (9)$$

and the corresponding eigenfrequencies,

$$\omega_{s\beta} = \sqrt{\frac{D_s}{\rho_s} \left\{ \left(\frac{\beta_1\pi}{L_{s1}}\right)^2 + \left(\frac{\beta_2\pi}{L_{s2}}\right)^2 \right\}}, \quad (10)$$

in which $\beta = (\beta_1, \beta_2)$ where β_1 and β_2 are positive integers. The finite dimension approximation of field u_s is written as $\tilde{u}_s(\omega, x, y) = \sum_{\beta \in \mathcal{B}^s} q_{s\beta}(\omega) \varphi_{s\beta}(x, y)$ in which \mathcal{B}^s is the set of all the pairs of integers (β_1, β_2) such that $\tilde{u}_s(\omega, x, y)$ approaches $u_s(\omega, x, y)$. As in Section I.A, we introduce vectors $\mathbf{q}_s(\omega)$ and $\mathbf{f}_s(\omega)$ such that

$$\mathbf{q}_s(\omega) = \{q_{s\beta}(\omega)\}_{\beta \in \mathcal{B}^s}, \quad \mathbf{f}_s(\omega) = \{f_{s\beta}(\omega)\}_{\beta \in \mathcal{B}^s}, \quad (11)$$

in which $f_{s\beta}(\omega) = \int_0^{L_{s1}} \int_0^{L_{s2}} f_s(\omega, x, y) \varphi_{s\beta}(x, y) dx dy$ and for all real ω , vector $\mathbf{q}_s(\omega)$ is the solution of the complex matrix equation $i\omega [Z_s(\omega)] \mathbf{q}_s(\omega) = \mathbf{f}_s(\omega)$ in which $[Z_s(\omega)]$ is the generalized impedance complex dense matrix such that

$$i\omega [Z_s(\omega)]_{\beta\beta'} = \rho_s \{-\omega^2 + 2i\omega \xi_s \omega_{s\beta} + \omega_{s\beta}^2\} \delta_{\beta\beta'} + z_s^\kappa(\omega) \varphi_{s\beta}(x^\kappa, y^\kappa) \varphi_{s\beta'}(x^\kappa, y^\kappa). \quad (12)$$

C. Generalized impedance matrix of the reference complex structure

The coupling between two plates of the master structure or between the master structure and a complex substructure is obtained by writing the continuity of rotations along the junctions (it should be noted that the continuity of the displacement field is satisfied). These resulting

linear constraint equations are then taken into account using Lagrange multipliers. Using the generalized impedance matrices introduced in Sections I.A and I.B yields

$$\begin{bmatrix} i\omega[Z_{\text{mast}}(\omega)] & 0 \\ 0 & i\omega[Z_{\text{sub}}(\omega)] \end{bmatrix} \begin{bmatrix} [B_{\text{mast}}]^T & [B_{\text{mast-sub}}]^T \\ 0 & [B_{\text{sub-mast}}]^T \end{bmatrix} \begin{bmatrix} \mathbf{q}_{\text{mast}}(\omega) \\ \mathbf{q}_{\text{sub}}(\omega) \\ \mathbf{p}_{\text{mast}}(\omega) \\ \mathbf{p}_{\text{sub}}(\omega) \end{bmatrix} = \begin{bmatrix} \mathbf{f}_{\text{mast}}(\omega) \\ 0 \\ 0 \\ 0 \end{bmatrix} \quad (13)$$

in which $\mathbf{q}_{\text{mast}}(\omega) = (\mathbf{q}_1(\omega), \mathbf{q}_2(\omega))$ and $\mathbf{q}_{\text{sub}}(\omega) = (\mathbf{q}_a(\omega), \mathbf{q}_b(\omega), \mathbf{q}_c(\omega), \mathbf{q}_d(\omega))$ are the vectors of the generalized coordinates of the master structure and the complex substructures respectively, and $\mathbf{p}_{\text{mast}}(\omega)$ and $\mathbf{p}_{\text{sub}}(\omega) = (\mathbf{p}_{1a}(\omega), \mathbf{p}_{1b}(\omega), \mathbf{p}_{2c}(\omega), \mathbf{p}_{2d}(\omega))$ are the vectors of the generalized coordinates of the Lagrange multipliers related to the coupling between the plates of the master structure and between the plates of the master structure and the complex substructures respectively. Finally, $\mathbf{f}_{\text{mast}}(\omega) = (\mathbf{f}_1(\omega), \mathbf{f}_2(\omega))$ is the vector of the generalized forces applied to the master structure. Impedance matrices $[Z_{\text{mast}}(\omega)]$ and $[Z_{\text{sub}}(\omega)]$ are written as

$$[Z_{\text{mast}}(\omega)] = \begin{bmatrix} [Z_1(\omega)] & 0 \\ 0 & [Z_2(\omega)] \end{bmatrix} \quad , \quad (14)$$

in which $[Z_1(\omega)]$ and $[Z_2(\omega)]$ are defined by Eq. (5) and

$$[Z_{\text{sub}}(\omega)] = \begin{bmatrix} [Z_a(\omega)] & 0 & 0 & 0 \\ 0 & [Z_b(\omega)] & 0 & 0 \\ 0 & 0 & [Z_c(\omega)] & 0 \\ 0 & 0 & 0 & [Z_d(\omega)] \end{bmatrix} \quad , \quad (15)$$

in which $[Z_a(\omega)]$, $[Z_b(\omega)]$, $[Z_c(\omega)]$ and $[Z_d(\omega)]$ are defined by Eq. (12). Finally, matrices $[B_{\text{mast}}]$, $[B_{\text{mast-sub}}]$ and $[B_{\text{sub-mast}}]$ are deduced²⁶ from the linear constraint equations introduced by the Lagrange multipliers. Equation (13) can be rewritten as

$$\begin{bmatrix} i\omega[Z(\omega)] & [B]^T \\ [B] & 0 \end{bmatrix} \begin{bmatrix} \mathbf{q}(\omega) \\ \mathbf{p}(\omega) \end{bmatrix} = \begin{bmatrix} \mathbf{f}(\omega) \\ 0 \end{bmatrix} \quad . \quad (16)$$

In general, and in particular for the reference complex structure under consideration, the matrix of Eq. (16) is not invertible due to redundant linear constraint equations induced by multiple connectivities. In order to circumvent this difficulty, we use a method²⁶ based on the use of the singular value decomposition of matrix $[B]$. This method allows the redundant equations to be automatically eliminated and Eq. (16) to be solved. Its solution $\mathbf{q}(\omega)$ is written as

$$\mathbf{q}(\omega) = [T(\omega)] \mathbf{f}(\omega) \quad , \quad (17)$$

D. Dynamical response of the reference complex structure

The response of the reference complex structure is obtained on the frequency band of analysis $[0, 1000]$ Hz. The plates of the master structure are identical. Each plate is homogeneous and isotropic with length $L_{r1} = 1$ m, width $L_{r2} = 0.5$ m, constant thickness 0.003 m, surface-mass density $\rho_r = 23.46$ kg/m², Young's modulus = 2.1×10^{11} N/m², Poisson's ratio 0.3, and constant damping rate $\xi_r = 0.003$. Each plate of the complex substructures is homogeneous and isotropic with constant thickness 0.002 m, surface-mass density $\rho_r = 15.64$ kg/m², Young's modulus = 2.1×10^{11} N/m², Poisson's ratio 0.3 and constant damping rate $\xi_r = 0.003$. The length and width of the plates of complex substructures (a) and (c) are equal to $L_{s1} = 1$ m and $L_{s2} = 0.5$ m respectively. The plates of complex substructures (b) and (d) are square and their length is equal to 0.5 m. In each complex substructure, there are 2401 oscillators having a total mass of 1 kg. The damping rate of each oscillator is equal to 0.003. The eigenfrequencies of the oscillators are uniformly distributed over frequency band $[0, 1000]$ Hz. The excitation force is applied to plate (1) at point located in $\mathbf{x}_0 = (0.707, 0.316)$, with a constant modulus equal to 1 N over the frequency band. The responses are calculated at point $\mathbf{x}_1 = (0.33, 0.166)$ in plate (1) and point $\mathbf{x}_2 = (0.48, 0.23)$ in plate (2). Figures 2 to 4 show the modulus (in dB) of frequency response function for the acceleration at points \mathbf{x}_0 , \mathbf{x}_1 and \mathbf{x}_2 of the master structure; the thin solid lines and the thick solid lines represent the response of the master structure uncoupled with the complex substructures and coupled with the complex substructures respectively. It should be noted that frequency band $[0, 300]$ Hz corresponds to the low-frequency range for which complex substructures do not significantly affect the responses of the master structure. In medium-frequency band $[300, 1000]$ Hz, the complex substructures play an important role in the response of the master structure, inducing an apparent strong damping in the master structure due to the power flow from the master structure to the structural complexity.

II. MODELING THE REFERENCE COMPLEX STRUCTURE USING THE FUZZY STRUCTURE THEORY

The fuzzy structure theory²³ is used to model the reference complex structure. The junctions between plate (1) of the master structure and its two attached fuzzy substructures (a) and (b) are denoted as $\Gamma_{1,\text{fuz}}^1$ and $\Gamma_{1,\text{fuz}}^2$ respectively. The junctions between plate (2) of the master

structure and its two attached fuzzy substructures (c) and (d) are denoted as $\Gamma_{2,\text{fuz}}^1$ and $\Gamma_{2,\text{fuz}}^2$ respectively (see Fig. 5).

A. Generalized impedance matrix of a master-structure plate coupled with its fuzzy substructures

Using the same notation as in Section I.A and denoting random displacement u_r as U_r , the boundary value problem related to plate (r) of the master structure coupled with its attached fuzzy substructures is written as

$$\begin{aligned} -\omega^2 \rho_r U_r - 2i\omega \xi_r (\rho_r D_r)^{1/2} \nabla^2 U_r + D_r \nabla^4 U_r &= f_r \quad \text{in } \Omega_r \quad , \\ U_r &= 0 \quad \text{on } \partial\Omega_r \quad , \\ \mathcal{M}_{\mathbf{n}_r} &= \mathcal{M}_{r,\text{fuz}}^1 \quad \text{on } \Gamma_{r,\text{fuz}}^1 \quad , \\ \mathcal{M}_{\mathbf{n}_r} &= \mathcal{M}_{r,\text{fuz}}^2 \quad \text{on } \Gamma_{r,\text{fuz}}^2 \quad , \\ \mathcal{M}_{\mathbf{n}_r} &= 0 \quad \text{on } \partial\Omega_r \setminus \{\Gamma_{r,\text{fuz}}^1 \cup \Gamma_{r,\text{fuz}}^2\} \quad , \end{aligned} \quad (18)$$

in which $\mathcal{M}_{r,\text{fuz}}^1$ and $\mathcal{M}_{r,\text{fuz}}^2$ are the moments induced by the two attached fuzzy substructures on plate (r) of the master structure. The fuzzy structure theory gives the expression of these moments $\mathcal{M}_{r,\text{fuz}}^\ell$ for $\ell = 1$ or 2,

$$\mathcal{M}_{r,\text{fuz}}^\ell(\omega; s) = \int_{\Gamma_{r,\text{fuz}}^\ell} i\omega Z_{r,\text{fuz}}^\ell(\omega; s, s') \frac{\partial U_r(\omega; s')}{\partial \mathbf{n}_r} ds' \quad , \quad (19)$$

in which random variable $Z_{r,\text{fuz}}^\ell(\omega; s, s')$ is written as

$$i\omega Z_{r,\text{fuz}}^\ell(\omega; s, s') = \{-\omega^2 S_{r,\text{fuz}}^\ell(\omega) + i\omega D_{r,\text{fuz}}^\ell(\omega)\} \delta_{\Gamma_{r,\text{fuz}}^\ell}(s' - s) \quad , \quad (20)$$

where $\delta_{\Gamma_{r,\text{fuz}}^\ell}$ is the Dirac function and where $\mathbb{Z}_{r,\text{fuz}}^\ell(\omega) = -\omega^2 S_{r,\text{fuz}}^\ell(\omega) + i\omega D_{r,\text{fuz}}^\ell(\omega)$ is the homogeneous fuzzy impedance law of fuzzy substructure ℓ such that

$$S_{r,\text{fuz}}^\ell(\omega) = S_{r,\text{mean}}^\ell(\omega) + \sum_{j=1}^4 X_{r,j}^\ell S_{r,j,\text{rand}}^\ell(\omega) \quad , \quad (21)$$

$$D_{r,\text{fuz}}^\ell(\omega) = D_{r,\text{mean}}^\ell(\omega) + \sum_{j=1}^4 X_{r,j}^\ell D_{r,j,\text{rand}}^\ell(\omega) \quad . \quad (22)$$

In Eqs. (21) and (22), $\{X_{r,1}^\ell, X_{r,2}^\ell, X_{r,3}^\ell, X_{r,4}^\ell\}$ are mutually independent second-order normalized random variables (centered and with a variance of 1) with a uniform probability distribution over $[-\sqrt{3}, \sqrt{3}]$ and

$$S_{r,\text{mean}}^\ell(\omega) = \omega \underline{\mu}_r^\ell \underline{n}_r^\ell \rho^R(\omega; \boldsymbol{\lambda}_r^\ell) \quad , \quad (23)$$

$$S_{r,1,\text{rand}}^\ell(\omega) = \omega \underline{\mu}_r^\ell \underline{n}_r^\ell \frac{\lambda_{r,1}^\ell}{\sqrt{3}} \rho^R(\omega; \boldsymbol{\lambda}_r^\ell) \quad , \quad (24)$$

$$S_{r,2,\text{rand}}^\ell(\omega) = \omega \underline{\mu}_r^\ell \underline{n}_r^\ell \frac{\sqrt{3}}{\lambda_{r,2}^\ell} \underline{\alpha}_r^\ell \underline{J}_5(\omega; \boldsymbol{\lambda}_r^\ell) \quad , \quad (25)$$

$$S_{r,3,\text{rand}}^\ell(\omega) = \omega \underline{\mu}_r^\ell \underline{n}_r^\ell \frac{\sqrt{3}}{\lambda_{r,3}^\ell} \underline{\alpha}_r^\ell \underline{J}_4(\omega; \boldsymbol{\lambda}_r^\ell) \quad , \quad (26)$$

$$S_{r,4,\text{rand}}^\ell(\omega) = \omega \underline{\mu}_r^\ell \underline{n}_r^\ell \frac{\lambda_{r,4}^\ell}{\sqrt{3}} \underline{\alpha}_r^\ell (\kappa_0(\omega) + \underline{J}_3(\omega; \boldsymbol{\lambda}_r^\ell)) \quad , \quad (27)$$

in which $\boldsymbol{\lambda}_r^\ell = (\lambda_{r,1}^\ell, \lambda_{r,2}^\ell, \lambda_{r,3}^\ell, \lambda_{r,4}^\ell)$ and

$$D_{r,\text{mean}}^\ell(\omega) = \frac{\pi}{2} \omega^2 \underline{\mu}_r^\ell \underline{n}_r^\ell \rho^I(\omega; \boldsymbol{\lambda}_r^\ell) \quad , \quad (28)$$

$$D_{r,1,\text{rand}}^\ell(\omega) = \frac{\pi}{2} \omega^2 \underline{\mu}_r^\ell \underline{n}_r^\ell \frac{\lambda_{r,1}^\ell}{\sqrt{3}} \rho^I(\omega; \boldsymbol{\lambda}_r^\ell) \quad , \quad (29)$$

$$D_{r,2,\text{rand}}^\ell(\omega) = \frac{\pi}{2} \omega^2 \underline{\mu}_r^\ell \underline{n}_r^\ell \frac{\sqrt{3}}{\lambda_{r,2}^\ell} [\kappa_1(\omega) \frac{\lambda_{r,2}^{\ell 2}}{3} (1 - \underline{\alpha}_r^\ell) + \underline{\alpha}_r^\ell \underline{J}_2(\omega; \boldsymbol{\lambda}_r^\ell)] \quad , \quad (30)$$

$$D_{r,3,\text{rand}}^\ell(\omega) = \frac{\pi}{2} \omega^2 \underline{\mu}_r^\ell \underline{n}_r^\ell \frac{\sqrt{3}}{\lambda_{r,3}^\ell} \underline{\alpha}_r^\ell \underline{J}_1(\omega; \boldsymbol{\lambda}_r^\ell) \quad , \quad (31)$$

$$D_{r,4,\text{rand}}^\ell(\omega) = \frac{\pi}{2} \omega^2 \underline{\mu}_r^\ell \underline{n}_r^\ell \frac{\lambda_{r,4}^\ell}{\sqrt{3}} \underline{\alpha}_r^\ell (\underline{J}_0(\omega; \boldsymbol{\lambda}_r^\ell) - \kappa_1(\omega)) \quad . \quad (32)$$

In Eqs. (23) to (32), functions ρ^R , ρ^I , κ_0 , κ_1 , \underline{J}_0 , \underline{J}_1 , \underline{J}_2 , \underline{J}_3 , \underline{J}_4 and \underline{J}_5 are explicitly defined in Appendix (Ref. 23, pages 368 to 370). The functions defined by Eqs. (23) to (32) depend on mean coefficients (or mean parameters) which are the mean coefficients of the participating inertial moment $\underline{\mu}_r^\ell(\omega)$, the mean rate of internal damping $\underline{\xi}_r^\ell(\omega)$, the mean modal density $\underline{n}_r^\ell(\omega)$ and the mean equivalent coupling factor $\underline{\alpha}_r^\ell(\omega)$ and their associated deviation coefficients $\lambda_{r,1}^\ell(\omega)$, $\lambda_{r,2}^\ell(\omega)$, $\lambda_{r,3}^\ell(\omega)$ and $\lambda_{r,4}^\ell(\omega)$ respectively. Mean coefficient $\underline{\mu}_r^\ell(\omega)$ is described by the dimensionless mean coefficient $\underline{\nu}_r^\ell(\omega)$ which is such that

$$\underline{\mu}_r^\ell(\omega) = \underline{\nu}_r^\ell(\omega) \frac{\mathcal{I}_r^\ell}{|\Gamma_{r,\text{fuz}}^\ell|} \quad , \quad (33)$$

in which \mathcal{I}_r^ℓ is an arbitrary reference inertial moment and $|\Gamma_{r,\text{fuz}}^\ell|$ is the measure of $\Gamma_{r,\text{fuz}}^\ell$ (equal to L_{r1} or L_{r2}). It is assumed that a direct estimation of mean coefficients $\underline{\xi}_r^\ell(\omega)$ and $\underline{n}_r^\ell(\omega)$ can be obtained. Since the junction between plate (r) of the master structure and fuzzy substructure ℓ is continuous, the fuzzy structure theory yields $\underline{\alpha}_r^\ell \ll 1$. In order to construct the generalized impedance matrix of plate (r) of the master structure coupled with its fuzzy substructures, we use the Ritz-Galerkin method introduced in Section I.A. The boundary value problem defined by Eq. (18) is then solved by introducing normal modes defined by Eq. (2) and their corresponding eigenfrequencies defined by Eq. (3). The finite dimension approximation of field U_r is again denoted as U_r and is written as

$$U_r(\omega, x, y) = \sum_{\beta \in \mathcal{B}^r} Q_{r\beta}(\omega) \varphi_{r\beta}(x, y) \quad . \quad (34)$$

As in section I.A, we introduce the vector $\mathbf{Q}_r(\omega)$ such that

$$\mathbf{Q}_r(\omega) = \{Q_{r\beta}(\omega)\}_{\beta \in \mathcal{B}^r} \quad , \quad (35)$$

and for all real ω , vector $\mathbf{Q}_r(\omega)$ is the solution of the complex matrix equation $i\omega ([Z_r(\omega)] + [Z_{r,\text{fuz}}(\omega)]) \mathbf{Q}_r(\omega) = \mathbf{f}_r(\omega)$ in which $[Z_r(\omega)]$ is given by Eq. (5) and $[Z_{r,\text{fuz}}(\omega)]$ is the generalized impedance complex dense matrix such that

$$[Z_{r,\text{fuz}}(\omega)]_{\beta\beta'} = [Z_{r,\text{mean}}(\omega)]_{\beta\beta'} + [Z_{r,\text{rand}}(\omega)]_{\beta\beta'} \quad , \quad (36)$$

in which

$$\begin{aligned} i\omega [Z_{r,\text{mean}}(\omega)]_{\beta\beta'} &= \sum_{\ell=1}^2 \{ -\omega^2 S_{r,\text{mean}}^\ell(\omega) + i\omega D_{r,\text{mean}}^\ell(\omega) \} \\ &\times \int_{\Gamma_{r,\text{fuz}}^\ell} \frac{\partial \varphi_{r\beta'}}{\partial \mathbf{n}_r}(s) \frac{\partial \varphi_{r\beta}}{\partial \mathbf{n}_r}(s) ds \quad , \end{aligned} \quad (37)$$

and

$$\begin{aligned} i\omega [Z_{r,\text{rand}}(\omega)]_{\beta\beta'} &= \sum_{\ell=1}^2 \sum_{j=1}^4 X_{r,j}^\ell \{ -\omega^2 S_{r,j,\text{rand}}^\ell(\omega) + i\omega D_{r,j,\text{rand}}^\ell(\omega) \} \\ &\times \int_{\Gamma_{r,\text{fuz}}^\ell} \frac{\partial \varphi_{r\beta'}}{\partial \mathbf{n}_r}(s) \frac{\partial \varphi_{r\beta}}{\partial \mathbf{n}_r}(s) ds \quad . \end{aligned} \quad (38)$$

B. Method for constructing the random response of the fuzzy structure

The coupling between the two plates of the master structure is written using Lagrange multipliers as in Section I.C. The generalized impedance matrix of the fuzzy structure is then written as

$$\begin{bmatrix} i\omega([Z_{\text{mast}}(\omega)] + [Z_{\text{mean}}(\omega)] + [Z_{\text{rand}}(\omega)]) & [B_{\text{mast}}]^T \\ & [B_{\text{mast}}] \end{bmatrix} \begin{bmatrix} \mathbf{Q}_{\text{mast}}(\omega) \\ \mathbf{P}_{\text{mast}}(\omega) \end{bmatrix} = \begin{bmatrix} \mathbf{f}_{\text{mast}}(\omega) \\ 0 \end{bmatrix}, \quad (39)$$

in which $[Z_{\text{mast}}(\omega)]$ is defined by Eq. (14), vector $\mathbf{Q}_{\text{mast}}(\omega)$ is such that

$$\mathbf{Q}_{\text{mast}}(\omega) = (\mathbf{Q}_1(\omega), \mathbf{Q}_2(\omega)) \quad , \quad (40)$$

in which $\mathbf{Q}_r(\omega)$ is defined by Eq. (35), $\mathbf{P}_{\text{mast}}(\omega)$ is the vector of the generalized coordinates of the Lagrange multipliers related to the coupling between the two plates of the master structure and where

$$[Z_{\text{mean}}(\omega)] = \begin{bmatrix} [Z_{1,\text{mean}}(\omega)] & 0 \\ 0 & [Z_{2,\text{mean}}(\omega)] \end{bmatrix} \quad , \quad (41)$$

$$[Z_{\text{rand}}(\omega)] = \begin{bmatrix} [Z_{1,\text{rand}}(\omega)] & 0 \\ 0 & [Z_{2,\text{rand}}(\omega)] \end{bmatrix} \quad , \quad (42)$$

in which $[Z_{r,\text{mean}}(\omega)]$ and $[Z_{r,\text{rand}}(\omega)]$ are defined by Eqs. (37) and (38) respectively. Equation (39) can be rewritten as

$$\begin{bmatrix} i\omega[Z_{\text{det}}(\omega)] + i\omega[Z_{\text{rand}}(\omega)] & [B_{\text{mast}}]^T \\ & [B_{\text{mast}}] \end{bmatrix} \begin{bmatrix} \mathbf{Q}_{\text{mast}}(\omega) \\ \mathbf{P}_{\text{mast}}(\omega) \end{bmatrix} = \begin{bmatrix} \mathbf{f}_{\text{mast}}(\omega) \\ 0 \end{bmatrix} \quad , \quad (43)$$

in which $[Z_{\text{det}}(\omega)] = [Z_{\text{mast}}(\omega)] + [Z_{\text{mean}}(\omega)]$ is a deterministic impedance matrix. The method used to solve Eq. (43) is based on the use of the Neumann series expansion. Consequently, we rewrite Eq. (43) as

$$\begin{bmatrix} i\omega[Z_{\text{det}}(\omega)] & [B_{\text{mast}}]^T \\ & [B_{\text{mast}}] \end{bmatrix} \begin{bmatrix} \mathbf{Q}_{\text{mast}}(\omega) \\ \mathbf{P}_{\text{mast}}(\omega) \end{bmatrix} = \begin{bmatrix} \mathbf{f}_{\text{mast}}(\omega) - i\omega[Z_{\text{rand}}(\omega)]\mathbf{Q}_{\text{mast}}(\omega) \\ 0 \end{bmatrix} \quad , \quad (44)$$

and the inverse matrix of the matrix appearing on the left-hand side of Eq. (44) is denoted as $[T_{\text{det}}(\omega)]$ (if this matrix is not invertible due to redundant equations induced by multiple connectivities in the master structure, then the method presented in Section I.C should be used

to construct $[T_{\det}(\omega)]$; for the present reference complex structure, since the master structure has only two plates, the matrix is invertible). We obtain the solution $\mathbf{Q}_{\text{mast}}(\omega)$ such that

$$\mathbf{Q}_{\text{mast}}(\omega) = [T_{\det}(\omega)](\mathbf{f}_{\text{mast}}(\omega) - i\omega[Z_{\text{rand}}(\omega)]\mathbf{Q}_{\text{mast}}(\omega)) \quad . \quad (45)$$

Equation (45) is rewritten as $([I_d] + i\omega[T_{\det}(\omega)][Z_{\text{rand}}(\omega)])\mathbf{Q}_{\text{mast}}(\omega) = [T_{\det}(\omega)]\mathbf{f}_{\text{mast}}(\omega)$ in which $[I_d]$ is the identity matrix. An approximation of the inverse of matrix $([I_d] + i\omega[T_{\det}(\omega)][Z_{\text{rand}}(\omega)])$ is calculated using Neumann's series expansion limited to order 2 and yields $([I_d] + i\omega[T_{\det}(\omega)][Z_{\text{rand}}(\omega)])^{-1} \simeq [I_d] + \sum_{k=1}^2 (-i\omega[T_{\det}(\omega)][Z_{\text{rand}}(\omega)])^k$. Solution $\mathbf{Q}_{\text{mast}}(\omega)$ can be written as

$$\mathbf{Q}_{\text{mast}}(\omega) = \mathbf{Q}_{\text{det}}(\omega) + \mathbf{Q}_{\text{rand}}(\omega) \quad , \quad (46)$$

in which

$$\mathbf{Q}_{\text{det}}(\omega) = [T_{\det}(\omega)]\mathbf{f}_{\text{mast}}(\omega) \quad , \quad (47)$$

$$\mathbf{Q}_{\text{rand}}(\omega) = \mathbf{Q}_{\text{rand}}^{(1)}(\omega) + \mathbf{Q}_{\text{rand}}^{(2)}(\omega) \quad , \quad (48)$$

with

$$\mathbf{Q}_{\text{rand}}^{(1)}(\omega) = -i\omega[T_{\det}(\omega)][Z_{\text{rand}}(\omega)]\mathbf{Q}_{\text{det}}(\omega) \quad , \quad (49)$$

$$\mathbf{Q}_{\text{rand}}^{(2)}(\omega) = -i\omega[T_{\det}(\omega)][Z_{\text{rand}}(\omega)]\mathbf{Q}_{\text{rand}}^{(1)}(\omega) \quad . \quad (50)$$

From Eqs. (34), (35), (40), (46) to (50), we deduce that in a point (x, y) of plate (r) of the master structure, the random response can be written as

$$U_r(\omega, x, y) = U_{r,\text{det}}(\omega, x, y) + U_{r,\text{rand}}(\omega, x, y) \quad , \quad (51)$$

$$U_{r,\text{rand}}(\omega, x, y) = \sum_{\ell=1}^{16} U_{r,\ell,\text{rand}}^{(1)}(\omega, x, y) X_{\ell} + \sum_{\ell=1}^{16} \sum_{\ell'=1}^{16} U_{r,\ell\ell',\text{rand}}^{(2)}(\omega, x, y) X_{\ell} X_{\ell'} \quad , \quad (52)$$

in which X_{ℓ} is the ℓ -th coordinate of vector $(X_{1,1}^1, \dots, X_{1,4}^1, \dots, X_{2,4}^2)$. The mean value and the variance of $U_r(\omega, x, y)$ are denoted as $E\{U_r(\omega, x, y)\}$ and $V_{U_r}(\omega, x, y)$ respectively and are defined by

$$E\{U_r(\omega, x, y)\} = U_{r,\text{det}}(\omega, x, y) + E\{U_{r,\text{rand}}(\omega, x, y)\} \quad , \quad (53)$$

and

$$V_{U_r}(\omega, x, y) = E\{|U_r(\omega, x, y) - E\{U_r(\omega, x, y)\}|^2\} \quad . \quad (54)$$

In order to get more information about the random response level $dB_r(\omega, x, y) = 20 \log_{10}(|U_r(\omega, x, y)|)$ of plate (r) expressed in dB, we construct the envelope of this random response in dB introducing the mean response level in dB

$$dB_r^0(\omega, x, y) = 20 \log_{10}(|E\{U_r(\omega, x, y)\}|) \quad . \quad (55)$$

The upper envelope $dB_r^+(\omega, x, y)$ is then defined by

$$\mathcal{P}(dB_r^-(\omega, x, y) < dB_r(\omega, x, y) \leq dB_r^+(\omega, x, y)) = P_c \quad , \quad (56)$$

in which the lower envelope is such that

$$dB_r^-(\omega, x, y) = 2 dB_r^0(\omega, x, y) - dB_r^+(\omega, x, y) \quad . \quad (57)$$

In Fig. 6, the gray region represents the confidence region defined by the upper and lower envelopes of the frequency-response-function modulus corresponding to a given probability level P_c . We construct the upper envelope using Chebychev's inequality which can be written as

$$\mathcal{P}(|U_r(\omega, x, y) - E\{U_r(\omega, x, y)\}| \geq a_r(\omega, x, y)) \leq \frac{V_{U_r}(\omega, x, y)}{a_r(\omega, x, y)^2} \quad , \quad (58)$$

in which $V_{U_r}(\omega, x, y)$ is given by Eq. (54). Inequality (58) yields

$$\mathcal{P}(dB_r^-(\omega, x, y) < dB_r(\omega, x, y) < dB_r^+(\omega, x, y)) \geq P_c \quad , \quad (59)$$

in which $dB_r^-(\omega, x, y)$ is defined by Eq. (57) and

$$dB_r^+(\omega, x, y) = 20 \log_{10}(|E\{U_r(\omega, x, y)\}| + a_r(\omega, x, y)) \quad , \quad (60)$$

in which $a_r(\omega, x, y)$ is such that

$$P_c = 1 - \frac{V_{U_r}(\omega, x, y)}{a_r(\omega, x, y)^2} \quad . \quad (61)$$

The confidence region calculated using the envelope defined by Eq. (59) is overestimated by comparison with a calculation made using Eq. (56), but the calculation is faster due to the use of an explicit numerical calculation of $E\{U_r(\omega, x, y)\}$ and $V_{U_r}(\omega, x, y)$.

III. ESTIMATION OF FUZZY STRUCTURE MEAN PARAMETERS

The fuzzy impedance law mean parameters $\underline{\alpha}_r^\ell$ and $\underline{\nu}_r^\ell$ of the fuzzy substructures introduced in Section II.A have to be estimated. Concerning mean parameter $\underline{\alpha}_r^\ell$, we know that $\underline{\alpha}_r^\ell \ll 1$ due to the continuous junctions. A sensitivity analysis with respect to this mean parameter was performed²⁷ and showed that the frequency-independent values

$$\underline{\alpha}_1^1 = \underline{\alpha}_1^2 = \underline{\alpha}_2^1 = \underline{\alpha}_2^2 = 0.005 \quad , \quad (62)$$

were a good approximation. Concerning mean parameter $\underline{\nu}_r^\ell$, we use the statistical energy approach introduced in Ref. 24 but using the following cost function²⁶

$$J(\underline{\nu}) = \sum_{r=1}^2 \left(\langle \Pi_{r,\text{diss}}(t; \underline{\nu}; 0) \rangle - \langle \Pi_{r,\text{diss}}^{\text{MSE}}(t) \rangle \right)^2 \quad , \quad (63)$$

in which $\underline{\nu} = (\nu_1^1, \nu_1^2, \nu_2^1, \nu_2^2)$; $\langle \Pi_{r,\text{diss}}(t; \underline{\nu}; 0) \rangle$ is the mean power dissipation in plate (r) of the master structure of the fuzzy structure, calculated using the fuzzy structure model; $\langle \Pi_{r,\text{diss}}^{\text{MSE}}(t) \rangle$ is the mean power dissipation in plate (r) of the master structure of the reference complex structure, estimated using statistical energy analysis applied to the reference complex structure. These mean power dissipations are calculated for a limited band time-stationary stochastic excitation force applied to the master structure²³. Consequently, the estimation $\underline{\nu}^*$ of $\underline{\nu}$ is given by solving the following optimization problem²⁶

$$J(\underline{\nu}^*) = \min_{\underline{\nu} \geq 0} J(\underline{\nu}) \quad , \quad (64)$$

in which $\underline{\nu} \geq 0$ means $\nu_1^1 \geq 0$, $\nu_1^2 \geq 0$, $\nu_2^1 \geq 0$ and $\nu_2^2 \geq 0$. The optimization problem defined by Eq. (64) is not easy to solve because cost function J is not convex and each evaluation of $J(\underline{\nu})$ needs an evaluation of $\langle \Pi_{r,\text{diss}}(t; \underline{\nu}; 0) \rangle$. Consequently, we developed²⁶ an algorithm with two main steps. In the first step, a neighborhood \mathcal{D} containing solution $\underline{\nu}^*$ is constructed using a random search algorithm. Domain \mathcal{D} is described by the polar coordinates $(\rho, \boldsymbol{\theta})$ such that

$$\underline{\nu} = \rho \frac{\boldsymbol{\theta}}{\|\boldsymbol{\theta}\|_2} \quad , \quad (65)$$

and is defined by

$$\mathcal{D} = \{\rho \in]\rho_{\min}, \rho_{\max}[, \boldsymbol{\theta} \in [0, 1]^4\} \quad . \quad (66)$$

The random search method is performed using a logarithmic scale for variable ρ . In Fig. 7, the gray region illustrates the \mathcal{D} region dimension 2. In the second step, the optimization problem defined by Eq. (64) is rewritten as

$$J(\underline{\mathbf{y}}^*) = \min_{\underline{\mathbf{y}} \in \mathcal{D}} J(\underline{\mathbf{y}}) \quad , \quad (67)$$

and is solved using Sequential Quadratic Programming²⁸ (SQP).

IV. VALIDATION

A. Description of the fuzzy structure modeling the reference complex structure

The frequency band of analysis is $B = [0, 1000]$ Hz. Band B is written as the union of 10 frequency sub-bands with a bandwidth of 100 Hz. Since the plate damping rate and the oscillator damping rates of each complex substructure are equal to 0.003, the mean rate of internal damping of each fuzzy substructure is taken equal to 0.003 over band B. The mean modal densities of the fuzzy substructures are equal to the mean modal densities of the systems constituted of the plates coupled with their attached oscillators. They are taken as constant over each frequency sub-band and are such that $\underline{n}_1^1 = \underline{n}_2^1 = 0.393$ s/rad and $\underline{n}_1^2 = \underline{n}_2^2 = 0.388$ s/rad. The mean equivalent coupling factors of the fuzzy substructures are such that $\underline{\alpha}_1^1 = \underline{\alpha}_1^2 = \underline{\alpha}_2^1 = \underline{\alpha}_2^2 = 0.005$ and are constant over band B. The arbitrary reference inertial moments of the fuzzy substructures are such that $\mathcal{I}_1^1 = \mathcal{I}_2^1 = 8.85$ kg \times m² and $\mathcal{I}_1^2 = \mathcal{I}_2^2 = 4.925$ kg \times m². Each mean coefficient of the participating inertial moment of a fuzzy substructure is taken as constant over each frequency sub-band. These mean coefficients are estimated using the method presented in Section III. The values obtained for $\underline{\nu}_1^1 \geq 0$, $\underline{\nu}_1^2 \geq 0$, $\underline{\nu}_2^1 \geq 0$ and $\underline{\nu}_2^2 \geq 0$, expressed in \log_{10} , are presented in Fig. 8 as a function of the frequency.

B. Mean response

We consider the mean response of the fuzzy structure with zero deviation coefficients. Figures 9 to 11 show the modulus (in dB) of the frequency response function for the acceleration at points \mathbf{x}_0 , \mathbf{x}_1 and \mathbf{x}_2 of the master structure; the thin solid lines represent the response of the reference complex structure and the thick solid lines represent the mean response of the fuzzy structure. It can be seen that the fuzzy structure's mean response with zero deviation coefficients gives a good representation of the reference complex structure response.

C. Envelopes

We consider the envelopes of the fuzzy structure response with nonzero deviation coefficients. The deviation coefficients associated with the participating inertial moments and the modal densities are nonzero and are taken as $\lambda_{1,1}^1 = \lambda_{1,1}^2 = \lambda_{2,1}^1 = \lambda_{2,1}^2 = \lambda_{1,3}^1 = \lambda_{1,3}^2 = \lambda_{2,3}^1 = \lambda_{2,3}^2 = 0.3$ whereas those associated with internal damping rates and equivalent coupling factors are taken equal to zero $\lambda_{1,2}^1 = \lambda_{1,2}^2 = \lambda_{2,2}^1 = \lambda_{2,2}^2 = \lambda_{1,4}^1 = \lambda_{1,4}^2 = \lambda_{2,4}^1 = \lambda_{2,4}^2 = 0$. Figures 12 to 14 show the modulus (in dB) of the frequency response function for the acceleration at points \mathbf{x}_0 , \mathbf{x}_1 and \mathbf{x}_2 of the master structure; the thick solid lines represent the response of the reference complex structure and the gray region represents the confidence region defined by the upper and lower envelopes predicted by the fuzzy structure theory and corresponding to a probability level equal to 0.95. It can be seen that the responses of the reference complex structure belong to this confidence region. Consequently, the prediction is satisfactory and this example validates the fuzzy structure theory for continuous junctions (line-couplings).

V. CONCLUSION

This paper constitutes a first validation of the fuzzy structure theory for continuous junctions (line-couplings) between the master structure and the fuzzy substructures. In particular, the capability of this theory to model fuzzy substructures constituted of local modes and equipment should be noted. The mean response function calculated by the fuzzy structure theory with zero deviation coefficients gives a good representation of the reference complex structure response and calculation of the envelopes with nonzero deviation coefficients based on the use of a second-order Neumann series expansion and Chebychev's inequality is very efficient. In addition, we have introduced a new cost function allowing estimation of the fuzzy structure parameters and we have proved that the statistical energy approach proposed in this procedure is very efficient. This procedure for estimating the fuzzy structure parameters, validated by numerical simulation, opens the field to experimental identifications.

APPENDIX: DEFINITIONS FOR THE FUNCTIONS IN EQS. (23) TO (32)

Function $\rho^R(\omega; \boldsymbol{\lambda}_r^\ell)$ is defined by

$$\rho^R(\omega; \boldsymbol{\lambda}_r^\ell) = (\underline{\alpha}_r^\ell - 1) \kappa_0(\omega; \boldsymbol{\lambda}_r^\ell) + \underline{\alpha}_r^\ell \underline{J}_3(\omega; \boldsymbol{\lambda}_r^\ell) \quad ,$$

$\kappa_0(\omega; \boldsymbol{\lambda}_r^\ell)$ is given by

$$\kappa_0(\omega; \boldsymbol{\lambda}_r^\ell) = [\omega \underline{n}_r^\ell]^{-1} + [12 \omega^3 \{\underline{n}_r^\ell\}^3 (1 - \{\lambda_{r,3}^\ell\}^2)]^{-1} \quad ,$$

function $\rho^I(\omega; \boldsymbol{\lambda}_r^\ell)$ is defined by

$$\rho^I(\omega; \boldsymbol{\lambda}_r^\ell) = (1 - \underline{\alpha}_r^\ell) \kappa_1(\omega; \boldsymbol{\lambda}_r^\ell) + \underline{\alpha}_r^\ell \underline{J}_0(\omega; \boldsymbol{\lambda}_r^\ell) \quad ,$$

$\kappa_1(\omega; \boldsymbol{\lambda}_r^\ell)$ is given by

$$\kappa_1(\omega; \boldsymbol{\lambda}_r^\ell) = 4 \underline{\xi}_r^\ell [\pi \omega \underline{n}_r^\ell]^{-1} \quad .$$

For $\kappa \in \{0, 1, 2, 3, 4, 5\}$, functions $\underline{J}_\kappa(\omega; \boldsymbol{\lambda}_r^\ell)$ are defined by

$$\underline{J}_\kappa(\omega; \boldsymbol{\lambda}_r^\ell) = \frac{1}{4} \int_{-1}^1 dy_2 \int_{-1}^1 dy_3 J_\kappa(\omega; \underline{\xi}_r^\ell (1 + \lambda_{r,2}^\ell y_2), \lambda_{r,3}^\ell y_3) \quad ,$$

with

$$J_0(\omega; x, y) = (1 + y) [\pi \sqrt{1 - x^2}]^{-1} [\arctan Y_+(\omega; x, y) - \arctan Y_-(\omega; x, y)] \quad ,$$

$$J_1(\omega; x, y) = y J_0(\omega; x, y) \quad ,$$

$$J_2(\omega; x, y) = (\underline{\xi}_r^\ell)^{-1} (x - \underline{\xi}_r^\ell) J_0(\omega; x, y) \quad ,$$

$$J_3(\omega; x, y) = [\omega \underline{n}_r^\ell]^{-1} - (1 + y) [4 \sqrt{1 - x^2}]^{-1} \ln[N(\omega; x, y)/D(\omega; x, y)] \quad ,$$

$$J_4(\omega; x, y) = y J_3(\omega; x, y) \quad ,$$

$$J_5(\omega; x, y) = (\underline{\xi}_r^\ell)^{-1} (x - \underline{\xi}_r^\ell) J_3(\omega; x, y) \quad .$$

Function $Y_\pm(\omega; x, y)$ is defined by

$$Y_\pm(\omega; x, y) = (\theta_\pm(\omega; y) + x^2) [x \sqrt{1 - x^2}]^{-1} \quad ,$$

in which

$$\theta_\pm(\omega; y) = [(1 \pm \tau(\omega; y))^2 - 1]/2 \quad ,$$

with

$$\tau(\omega; y) = [2 \omega \underline{n}_r^\ell (1 + y)]^{-1} \quad .$$

Functions $N(\omega; x, y)$ and $D(\omega; x, y)$ are defined by

$$N(\omega; x, y) = [U_+(\omega; y) + W_+(\omega; x, y)][U_-(\omega; y) - W_-(\omega; x, y)] \quad ,$$

$$D(\omega; x, y) = [U_+(\omega; y) - W_+(\omega; x, y)][U_-(\omega; y) + W_-(\omega; x, y)] \quad ,$$

in which

$$U_{\pm}(\omega; y) = 2 (\theta_{\pm}(\omega; y) + 1) \quad ,$$

$$W_{\pm}(\omega; x, y) = 2 \sqrt{1 - x^2} [1 \pm \tau(\omega; y)] \quad .$$

- ¹ C. Soize, "Probabilistic structural modeling in linear dynamic analysis of complex mechanical systems. I- Theoretical elements," *La Recherche Aéronautique* **5**, 23–48, (1986). (English edition).
- ² C. Soize, "A model and numerical method in the medium frequency range for vibroacoustic predictions using the theory of structural fuzzy," *J. Acoust. Soc. Am.* **94**(2), 849–865 (1993).
- ³ V.W. Sparrow, D.A. Russel and J.L. Rochat, "Implementation of discrete fuzzy structure models in mathematica," *Int. J. Numer. Methods Eng.* **37**, 3005–3014 (1994).
- ⁴ D. Trentin and J.L. Guyader, "Vibration of a master plate with attached masses using modal sampling method," *J. Acoust. Soc. Am.* **96**(1), 235–245 (1994).
- ⁵ G. Maidanik, "Power dissipation in a sprung mass attached to a master structure," *J. Acoust. Soc. Am* **98**(3), 3527–3533 (1995).
- ⁶ A.D. Pierce, V.W. Sparrow and D.A. Russel, "Fundamental Structural-Acoustic Idealizations for Structures with Fuzzy Internal," *Journal of Vibration and Acoustics* **117**, 339–348 (1995).
- ⁷ D.A. Russel, *The Theory of Fuzzy Structures and its Application to Waves in Plates and Shells* (Ph.D dissertation at Pennsylvania State University, Graduate Program in Acoustics, State College PA, 1995).
- ⁸ D.A. Russel and V.W. Sparrow, "Backscattering from a baffled finite plate strip with fuzzy attachments," *J. Acoust. Soc. Am.* **98**(3), 1527–533 (1995).
- ⁹ G. Maidanik and J. Dickey, "Design criteria for the damping effectiveness of structural fuzzies," *J. Acoust. Soc. Am* **100**(4), 2029–2033 (1996).
- ¹⁰ M. Strasberg and D. Feit, "Vibration damping of large structures induced by attached small resonant structures," *J. Acoust. Soc. Am.* **99**(1), 335–344 (1996).
- ¹¹ R.L. Weaver, "The effect of an undamped finite degree of freedom "fuzzy" substructure: Numerical solutions and theoretical discussion," *J. Acoust. Soc. Am.* **100**(5), 3159–3164 (1996).
- ¹² Y.K. Lin, "On the standard deviation of change-in-impedance due to fuzzy subsystems," *J. Acoust. Soc. Am.* **101**(1), 616–618 (1997).
- ¹³ D.M. Photiadis, J.A. Bucaro and B.H. Houston, "The effect of internal oscillators on the acoustic response of a submerged shell," *J. Acoust. Soc. Am* **101**(2), 895–899 (1997).
- ¹⁴ A.D. Pierce, "Resonant-frequency-distribution of internal mass inferred from mechanical impedance matrices, with application to fuzzy structure theory," *ASME Paper 93-WA/NCA-*

- 17, 1993, also published in *Journal of Vibration and Sound* **119**, 324–333 (1997).
- ¹⁵ R.L. Weaver, “Mean and mean-square responses of a prototypical master/fuzzy structure,” *J. Acoust. Soc. Am.* **101**(3), 1441–1449 (1997).
- ¹⁶ A. Cherukuri and P.E. Barbone, “High modal density approximations for equipment in the time domain,” *J. Acoust. Soc. Am.* **104**(4), 2048–2053 (1998).
- ¹⁷ G. Maidanik and K.J. Becker, “Various loss factors of a master harmonic oscillator coupled to a number of satellite harmonic oscillators,” *J. Acoust. Soc. Am.* **103**(6), 3184–3195 (1998).
- ¹⁸ N.J. Tarp-Johansen, O. Ditlevsen and Y.K. Lin, “Secondary systems modeled as fuzzy substructures,” *Structural Safety & Reliability*, Shiraishi, Shinozuka & Wen (eds), 803–810, Balkema, Rotterdam (1998).
- ¹⁹ G. Maidanik and J. Dickey, “An impulse response function for a fuzzy structure,” *J. Acoust. Soc. Am.* **97**(3), 1460–1476 (1995).
- ²⁰ J. Garrelick, “The modeling of a continuous structure as a fuzzy,” *J. Acoust. Soc. Am.* **101**(1), 613–615 (1997).
- ²¹ J.J. MacCoy and B.Z. Steinberg, “Addressing complexity in structural acoustics-fuzzy structure and effective impedance theories,” *Computers and Structures* **65**(3), 403–421 (1997).
- ²² R.S. Langley and P. Bremmer, “A hybrid method for the vibration analysis of complex structural-acoustic systems,” *J. Acoust. Soc. Am.* **105**(3), 1657–1672 (1999).
- ²³ R. Ohayon and C. Soize, *Structural Acoustics and Vibration* (Academic Press, San Diego, 1998).
- ²⁴ C. Soize, “Estimation of the fuzzy substructure model parameters using the mean power flow equation of the fuzzy structure,” *Proceeding of the ASME Noise Control and Acoustics Divisions*, Volume 1, ASME/WAM, 28–30, NCA-Vol. 22, 23–30 (1996), also published in *Journal of Vibration and Acoustic* **120**(1), 279–286 (1998).
- ²⁵ A. Leissa, *Vibration of Plates and Vibration of Shells* (Acoust. Soc. Am. Publications on Acoustics, Woodbury, 1993). Originally published by NASA, 1973.
- ²⁶ R. Ohayon, R. Sampaio and C. Soize, “Dynamic substructuring of damped structures using singular value decomposition,” *Journal of Applied Mechanics* **64**, 292–298 (1997).
- ²⁷ K. Bjaoui, *Estimation des paramètres d’une structure floue pour des jonctions continues* (Thèse du Conservatoire National des Arts et Métiers, Paris, 1999).
- ²⁸ R. Fletcher, *Practical Methods of Optimization, vol. 2, Constrained Optimization* (John Wiley

and Sons., 1980).

²⁹ A.Y.T. Leung, *Dynamic Stiffness and Substructures* (Springer-Verlag, New-York, 1993).

³⁰ R. MacNeal, "A hybrid method of component mode synthesis," *Computers and Structures* **1**, 581–601 (1971).

LEGENDS ACCOMPANYING EACH FIGURE

FIG. 1. Reference complex structure.

FIG. 2. Modulus (in dB) of the frequency response function for the acceleration at point \mathbf{x}_0 of the master structure: master structure not coupled with the complex substructures (thin solid line); master structure coupled with the complex substructures (thick solid line).

FIG. 3. Modulus (in dB) of the frequency response function for the acceleration at point \mathbf{x}_1 of the master structure: master structure not coupled with the complex substructures (thin solid line); master structure coupled with the complex substructures (thick solid line).

FIG. 4. Modulus (in dB) of the frequency response function for the acceleration at point \mathbf{x}_2 of the master structure: master structure not coupled with the complex substructures (thin solid line); master structure coupled with the complex substructures (thick solid line).

FIG. 5. Model of the reference complex structure by fuzzy structure theory.

FIG. 6. Confidence region defined by the upper and lower envelopes of the frequency-response-function modulus corresponding to a given probability level.

FIG. 7. Geometrical shape of the domain in which the solution of the optimization problem belongs.

FIG. 8. Dimensionless mean coefficients $\underline{\nu}$ in \log_{10} : mean coefficient $\underline{\nu}_1^1$ (thin solid line); mean coefficient $\underline{\nu}_1^2$ (thin dashed line); mean coefficient $\underline{\nu}_2^1$ (thick solid line); mean coefficient $\underline{\nu}_2^2$ (thick dashed line).

FIG. 9. Modulus (in dB) of the frequency response function for the acceleration at point \mathbf{x}_0 of the master structure: response of the reference complex structure (thin solid line); mean response of the fuzzy structure (thick solid line).

FIG. 10. Modulus (in dB) of the frequency response function for the acceleration at point \mathbf{x}_1 of the master structure: response of the reference complex structure (thin solid line); mean response of the fuzzy structure (thick solid line).

FIG. 11. Modulus (in dB) of the frequency response function for the acceleration at point \mathbf{x}_2 of the master structure: response of the reference complex structure (thin solid line); mean response of the fuzzy structure (thick solid line).

FIG. 12. Modulus (in dB) of the frequency response function for the acceleration at point \mathbf{x}_0 of the master structure: response of the reference complex structure (thick solid line);

confidence region defined by the upper and lower envelopes predicted by the fuzzy structure theory and corresponding to a probability level equal to 0.95.

FIG. 13. Modulus (in dB) of the frequency response function for the acceleration at point \mathbf{x}_1 of the master structure: response of the reference complex structure (thick solid line); confidence region defined by the upper and lower envelopes predicted by the fuzzy structure theory and corresponding to a probability level equal to 0.95.

FIG. 14. Modulus (in dB) of the frequency response function for the acceleration at point \mathbf{x}_2 of the master structure: response of the reference complex structure (thick solid line); confidence region defined by the upper and lower envelopes predicted by the fuzzy structure theory and corresponding to a probability level equal to 0.95.

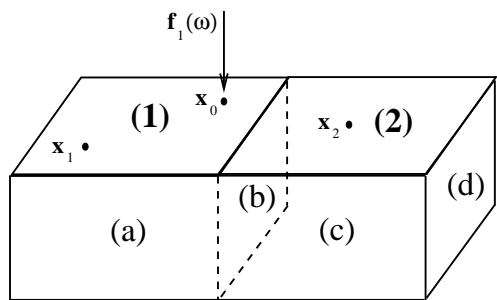


Fig. 1, C. Soize and K. Bjaoui, J. Acoust. Soc. Am.

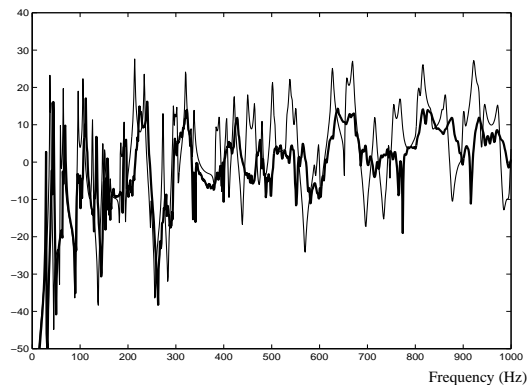


Fig. 4, C. Soize and K. Bjaoui, J. Acoust. Soc. Am.

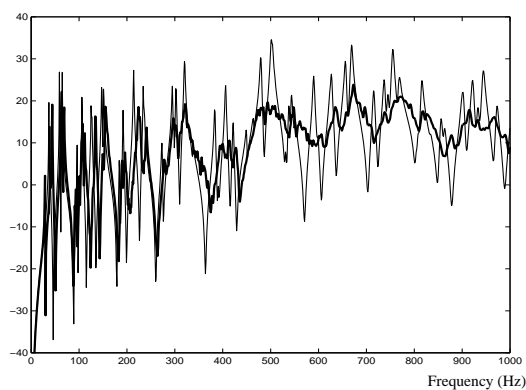


Fig. 2, C. Soize and K. Bjaoui, Acoust. Soc. Am.

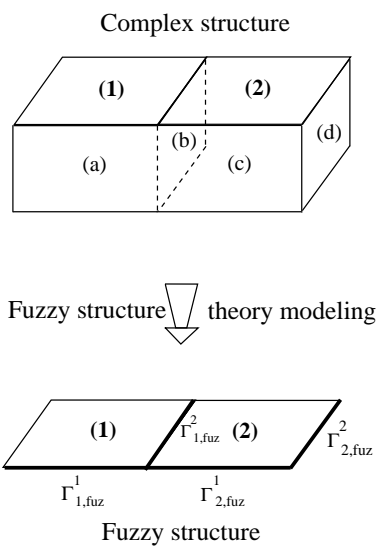


Fig. 5, C. Soize and K. Bjaoui, J. Acoust. Soc. Am.

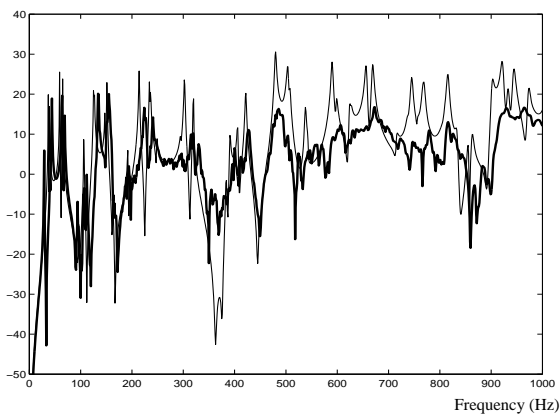


Fig. 3, C. Soize and K. Bjaoui, J. Acoust. Soc. Am.

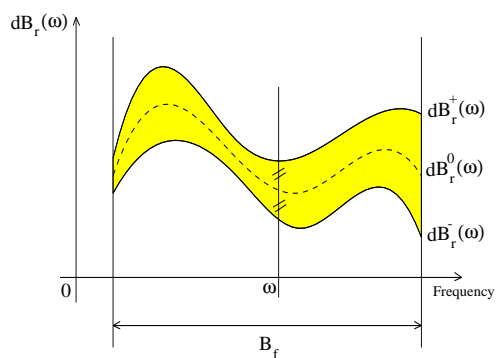


Fig. 6, C. Soize and K. Bjaoui, J. Acoust. Soc. Am.

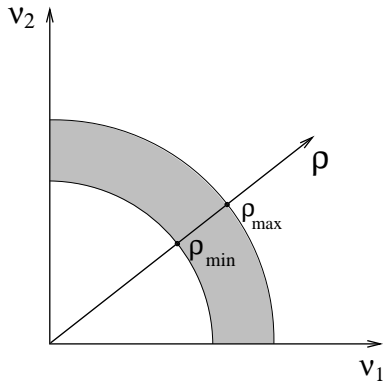


Fig. 7, C. Soize and K. Bjaoui, J. Acoust. Soc. Am.

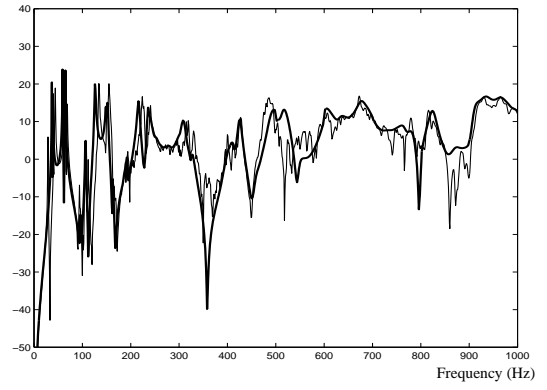


Fig. 10, C. Soize and K. Bjaoui, J. Acoust. Soc. Am.

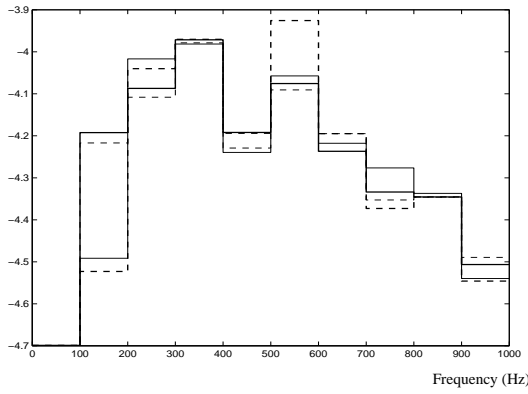


Fig. 8, C. Soize and K. Bjaoui, J. Acoust. Soc. Am.

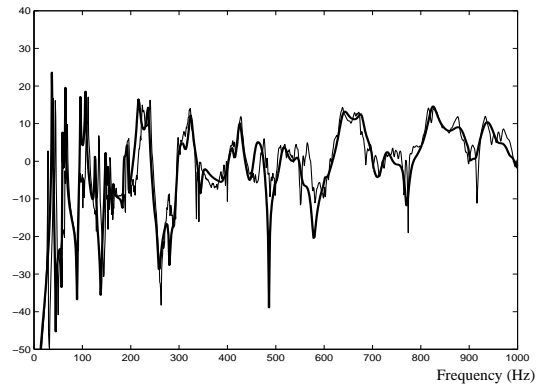


Fig. 11, C. Soize and K. Bjaoui, J. Acoust. Soc. Am.

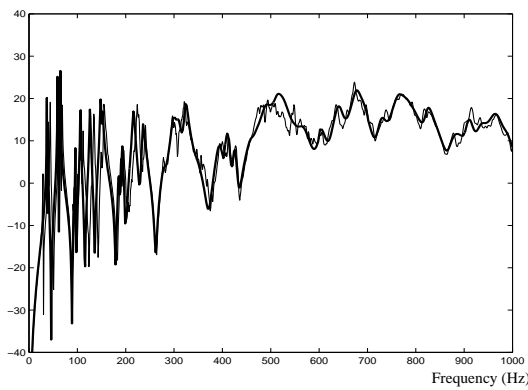


Fig. 9, C. Soize and K. Bjaoui, J. Acoust. Soc. Am.

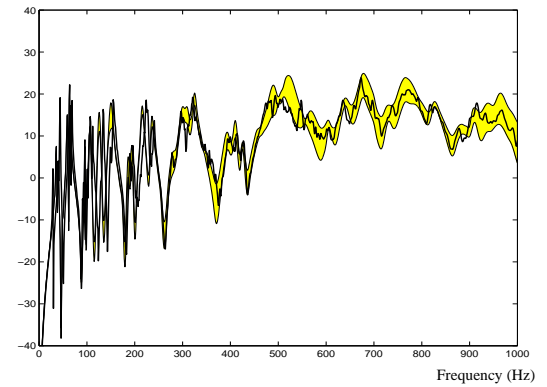


Fig. 12, C. Soize and K. Bjaoui, J. Acoust. Soc. Am.

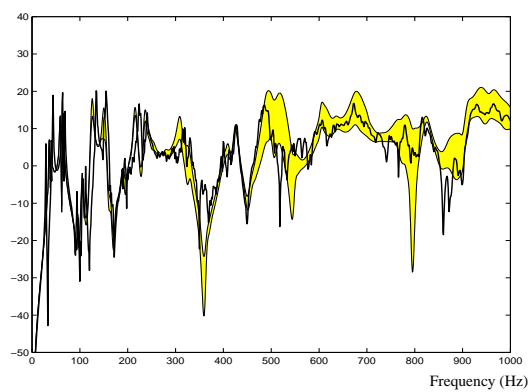


Fig. 13, C. Soize and K. Bjaoui, J. Acoust. Soc. Am.

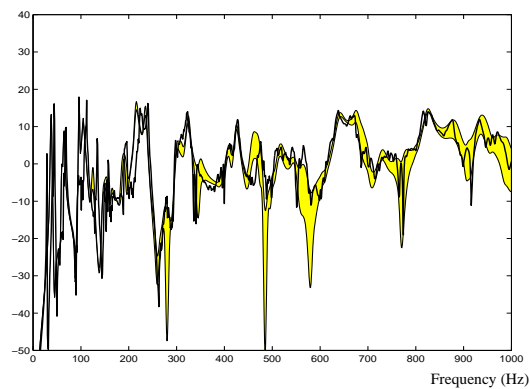


Fig. 14, C. Soize and K. Bjaoui, J. Acoust. Soc. Am.